National Seminar on Application of Artificial Intelligence in Life Sciences (NSAAILS - 2013)
Proceedings published in International Journal of Computer Applications® (IJCA) (0975 – 8887)

Structural and Dynamic Insights into S100B Protein Activity Inhibition by Melittin for the Treatment of Epilepsy

Neeraj Verma
The Bioinformatica Solutions,
Society for Biological Research & Rural Development, Lucknow 226024 India

Madhumita Karmakar
Department of Bioinformatics, System Toxicology Group,
CSIR-Indian Institute of Toxicology Research, Lucknow 226001 India.

Krishna P Singh
Department of Bioinformatics, System Toxicology Group,
CSIR-Indian Institute of Toxicology Research, Lucknow 226001 India.

Suchi Smita*
The Bioinformatica Solutions,
Society for Biological Research & Rural Development, Lucknow 226024 India

* Corresponding Author

ABSTRACT

Epilepsy is a common chronic central nervous system disorder characterized by repeated malicious seizures. Current medications acceptable by medical practitioners till date mostly suppresses the seizures and has symptomatic relief, but no effect on epileptogenesis. In the present work, we have attempted to provide the scientific base to use the bee venom therapy (Apitherapy) which was practiced throughout ancient Egyptian, Greek and Chinese civilization to treat epilepsy. Our computational studies and molecular dynamics simulation results indicate that interaction between S100B (calcium binding protein) and melittin (a venom peptide from bee), resulted in the structural distortion and inaccessibility of calcium binding domain of S100B protein, which is required to maintain ionic imbalance due to over expressed S100B in disease conditions.

General Terms

Nervous System Disorder, Apitherapy, Molecular Dynamics Simulation

Keywords

Epilepsy, Melittin, S100B, Protein-Protein Interaction, Ca^{2+} - binding domains

1. INTRODUCTION

Epilepsy is a neuronal disorder in which person has repeated convulsions because of enormous disruption of electrical communication between neurons in the brain, leading to the temporary release of excessive energy in a coordinated form [1]. Worldwide over 50 million people are affected by epilepsy of which 80% resides in developing countries [2]. Epileptic disorders have been treated with a variety of botanicals and herbs for thousands of years that include extracts from kava, valerian, chamomile, passionflower etc [3]. In ancient Indian medicine system, uses of powdered beans with wine or water were considered as a highly valued remedy for epilepsy. Several new drugs viz. Felbamate, Gabapentin, Lamotrigine, Topiramate, Tiagabine, Levetiracetam, Oxcarbazepine and many more have also been stamped in last two decades [4, 5, 6]. Despites of such a huge list of anti-epileptic compound, currently there is no drug available which can prevent epileptogenesis [7, 8, 9]. In most of the cases patient usually requires polytherapy. However, there are few reports where complete symptomatic relief has been observed in the epileptic patients after bee venom therapy.

The bee venom is a rich source of several biologically active components of which melittin, apamin, adolpin, phospholipase A2 have been studied in details [10]. Melittin, the main elementary and hydrophobic peptide represents 50-60% of the total amount of the chemical constituents of Apis mellifera venom [11, 12]. Epilepsy is the disease state resulted by the hyper excitability (firing and burst) of neurons due to the interruption in the flow of calcium, sodium and potassium ions through voltage and ligand-gated ion channels. Voltage gated calcium and potassium ion channels plays a significant role in different biological processes, including neurotransmitter release, excitation-contraction of muscle and regulation of gene expression as well as neuronal migration. In addition, compounds that directly affect Ca^{++}/ K^{+} channels or proteins that modulate their activity are used to treat a number of neurological pathologies [13]. In case of epilepsy, over expression of S100B, a calcium binding protein has been observed throughout the epileptic development process. S100B, a sub protein of S100 protein family, are localized in cytoplasm and nucleus of vast range of cells implicated in the regulation of a number of cellular processes such as cell cycle progression, separation and their association in several human diseases such as rheumatoid arthritis, acute inflammatory lesions, cardiomyophathy, Alzheimer's disease, and cancer [14, 15]. It has been suggested that the down regulation of S100B has a potential in epileptic therapy [16]. The interaction of Melittin with S100B protein was previously observed in the presence and absence of calcium by fluorescence polarization, UV difference spectroscopy, and sulfhydryl derivatization [17, 18], which establish melittin as potential therapeutic agent in case of epilepsy.

2. MATERIALS AND METHODS

The three dimensional (3D) structural data of melittin (PDB: 2MLT) and S100B (PDB: 2H61) was retrieved from the Protein Data Bank available at www.rcsb.org. The protein structures were cleaned using Prepare Protein tools of Accelerys Discovery Studio (DS) 3.1. These tools correct structural disorders, nonstandard names for amino acid residues, incomplete residues, protein residue connectivity and bond orders, missing side-chain or backbone atoms, addition of hydrogen atoms and other errors. CHARMm (Chemistry at HARvard Macromolecular Mechanics) forcefield, a semi empirical quantum-chemistry program and a modular quantum-mechanical/mole quantum (QM/MM) package [19] was assigned to the molecules before being subjected to molecular docking studies.

The intermolecular interactions between S100B and melittin proteins were studied through molecular docking approach. This task was attained using ZDock and RDock programs of DS3.1. The ZDOCK protocol provides rigid body docking of two protein structures using the ZDOCK algorithm [20] as well as clusters the poses according to the ligand position. The free energy change upon binding of ligand to a receptor is calculated as:

$$\Delta G_{desolv} = W_{desolv} \sum_{i,j} (S_i V_j + S_j V_i)\, e^{\frac{-r_{ij}^2}{2\sigma^2}}$$

where i = index of atoms in the ligand, j = index of atoms in the receptor, W_{desolv} = linear regression coefficient or weight for the desolvation free energy term, S_i = solvation term for atom i, V_i = atomic fragmental volume of atom i, r_{ij} = distance between atom i and atom j (in Å) and σ = Gaussian distance constant = 3.5 Å.

In the initial stage, the protein and peptide molecules were treated as rigid bodies and all six revolving and translational degrees of freedom were entirely explored with the scoring functions that are liberal to conformational changes [21]. The predicted docked structures from ZDOCK were refined and re-ranked in order to pick out near-native structures using RDOCK [22] program. The program is mainly a two-stage energy minimization scheme that includes evaluation of electrostatic and desolvation energies. It takes advantage of CHARMm [23] to remove clashes and optimize polar and charge interactions. For 2-stage energy-minimization and optimization in RDOCK, each ZDOCK prediction was run through 130 steps of Adopted Basis Newton-Raphson (ABNR) energy minimization using the CHARMm forcefield [24]. In the first stage of optimization, all the clashes between the atoms were removed by allowing atoms to move freely followed by total energy minimization (which is the sum of coulombic electrostatics, vdW, and internal energies) of the complex. During this stage, ionic side-chains were kept at their neutral states and non-hydrogen atoms were restrained harmonically at their starting positions with a mass-weighted force constant of 20 kcal/ (mol*Å). In the second stage of minimization in RDOCK, all ionic residues were kept in their charged states and the structures were subjected to energy minimization without any constraints. All the complex structures with vdW energies higher than 10 kcal/mol were penalized and considered as no hits. The desolvation energies of all the filtered structures were computed after both steps of minimization using the Atomic Contact Energy (ACE) algorithm [21]. The desolvation energy of forming a protein complex (〖ΔG〗_ACE) from individual receptor and ligand structures is the sum of the atomic ACE scores of all receptor-ligand atom pairs within a distance cutoff of 6 angstroms. The scoring function of RDOCK is calculated as the sum of ACE desolvation energy (〖ΔG〗_ACE) and the CHARMm electrostatics energy (〖ΔE〗_elec) [21] using following equation:

〖ΔG〗_binding= 〖ΔG〗_ACE+ β × 〖ΔE〗_elec

where β is a scaling factor (default value = 0.9).

In order to evaluate the relative stability of several interaction poses generated between melittin and S100B, we used molecular dynamics (MD) simulations using CHARMm force field. CHARMm uses a flexible empirical energy function that is summation of many individuals' energy terms. Each energy function is based on internal co-ordinates and pair-wise non-bonded interaction terms. The total energy term (E_pot) is calculated by following equation:

E_pot = (E_bond + E_angle + E_torsion + E_oop + E_electrostatic + E_vdW + E_constraint + E_user)

where, the OOP (out-of-plane) angle is defined as an improper torsion [23]. For each interaction pose, configuration of the docked structure with lowest electrostatic interaction energy after RDOCK refinement was used as the starting structure for MD simulation using Standard Dynamics Cascade of DS 3.1. Energy minimization was performed to obtain the stable initial structure by applying 500 steps of steepest decent algorithm followed by 500 steps of conjugate gradient method. NVT condition i.e. constant number of particles, volume and temperature was maintained during the whole simulation process. Equilibration of the whole system was carried out for 1000 ps followed by heating period of 2000 ps. Finally, the 5 ns of production run were attained with a time step of 1 fs. The target temperature was set to 300 K, using a coupling constant (T_T) of 0.1 ps.

3. RESULTS

3.1 Molecular docking of S100B and Melittin proteins

The 3D structural files of S100B and melittin were downloaded from the Protein Data Bank (www.rcsb.org). To prepare the structures for molecular docking, water molecules were removed from the pdb files. The protein – protein interaction between S100B and melittin was performed using ZDOCK protocol available in Accelrys Discovery Studio 3.1. S100B, a calcium binding protein (PDB: 2H61), was chosen as a receptor and melittin peptide (PDB: 2MLT) was selected as ligand. Both the receptor and ligand proteins were typed with CHARMm Polar H force field and the dielectric constant parameter was set to 4.0. The angular step size was set to 6 as this search provides more accurate predictions. Both RMSD and Interface cut-off were set as 10.0. Maximum 20 clusters were allowed to form and Rest parameters were set as default values. With all these parameters, protein-protein interaction poses were generated. Docked poses with high ZDOCK scores, high density values and low cluster numbers were selected for the refinements. In our case, a total of 20 clusters were formed covering all the possible interaction poses between two proteins. Cluster-1, the largest cluster, contains 16 docked poses, followed by progressively smaller clusters.

The best 20 poses chosen on the basis of ZDOCK score were selected for further refining and analysis (Table 1).

Table.1: ZDock result table showing important features of top 20 poses for interaction of S100B with melittin

Pose No.	X *	Y *	Z *	Cluster	Cluster size	Density	Zdock score
Pose19	-4.556	-5.484	24.105	2	10	5	12.56
Pose17	-15.604	-0.983	32.468	1	16	16	12.08
Pose14	-15.488	-0.041	31.453	1	16	16	12.06
Pose95	-15.718	-1.115	32.315	1	16	16	12
Pose47	-5.678	-7.263	25.572	2	10	5	11.92
Pose29	-15.598	-1.141	32.468	1	16	16	11.82
Pose89	-14.288	0.105	31.446	1	16	16	11.7
Pose67	7.311	-20.673	41.669	3	9	9	11.68
Pose18	-15.452	-0.406	31.678	1	16	16	11.64
Pose65	7.213	-20.509	41.669	3	9	9	11.46
Pose23	-15.598	-1.314	31.286	1	16	16	11.44
Pose39	-14.229	-5.295	28.298	7	4	4	11.32
Pose4	-7.874	-1.509	28.395	2	10	6	11.28
Pose9	-15.586	-1.155	31.286	1	16	16	11.18
Pose60	6.079	-20.585	42.035	3	9	9	11.02
Pose59	7.181	-20.502	41.541	3	9	9	10.96
Pose20	-15.51	-0.209	31.453	1	16	16	10.9
Pose30	-16.201	2.152	33.413	10	3	3	10.86
Pose66	-4.628	-5.437	23.975	2	10	5	10.78
Pose54	-15.41	-0.23	31.678	1	16	16	10.72

* X / Y / Z are the coordinates of various poses in the interaction file.

3.2 Refinement of ZDock results using RDock program

Refinement of top 20 docked poses obtained from ZDOCK was achieved using RDOCK algorithm [19] which uses a CHARMm-based technique for refinement and scoring. Total 2 step energy minimizations were carried out using RDOCK. During first minimization step, the electrostatics energy (Elec) was calculated using CHARMm with a distance dependent dielectric constant, and for the second stage minimization, keeping all ionic side chains in their full charge states. The refined poses were arranged on the basis of E_RDOCK score (Table 2). After RDock refinement, pose 30 was identified as the best pose showing lowest E_RDOCK and van der Waals energy of -44.388 and -60.942 respectively. The interaction of S100B and Melittin in pose 30 is shown in Figure 1.

A total of 6 inter-molecular hydrogen bonds were formed between S100B and melittin that are responsible for the stability of complex. Atoms of receptor and ligand whose distance is less than or equal to a threshold are considered as Bumps in the molecular interactions. Bump monitors attempt to approximate the existence of hydrogen atoms if valences are not filled.

Table 2. Various energy parameters of S100B and melittin interaction poses after RDOCK refinement.

Name	E_ RDOCK	E_elec1	E_elec2	E_sol	E_vdw1	E_vdw2
Pose30	-44.388	-0.0591	-41.0978	-7.4	-48.6899	-60.942
Pose4	-37.7935	0.089745	-34.9928	-6.3	-62.6273	-61.8091
Pose95	-37.0824	-2.03008	-26.6471	-13.1	-41.0805	-63.4353
Pose29	-33.9079	-0.94568	-23.3421	-12.9	-60.6649	-66.3708
Pose17	-31.9651	-2.08025	-20.8501	-13.2	-55.7366	-68.0333
Pose39	-30.8498	0.060568	-14.2775	-18	-65.0798	-75.8816
Pose18	-29.4344	-2.08173	-23.2604	-8.5	-60.0005	-64.5498
Pose89	-29.1075	-0.48631	-19.675	-11.4	-65.2512	-63.6709
Pose23	-28.505	0.616019	-20.3389	-10.2	-65.712	-73.3751
Pose20	-27.2998	-2.24908	-21.6664	-7.8	-65.5325	-66.951
Pose9	-26.3893	0.604779	-18.3214	-9.9	-68.3098	-71.2363
Pose54	-26.0109	-1.22943	-20.0121	-8	-59.7462	-64.2974
Pose14	-25.7337	-2.01935	-20.1486	-7.6	-67.6252	-67.449
Pose19	-23.4601	3.28496	-14.6223	-10.3	-62.6205	-65.2999
Pose66	-23.1371	1.81767	-15.4857	-9.2	-68.5456	-74.3126
Pose47	-21.4577	5.44383	-13.1752	-9.6	-69.3362	-71.5381
Pose60	-19.5074	-0.59674	-7.89716	-12.4	-62.045	-61.4026
Pose59	-17.3507	-0.75821	-7.61192	-10.5	-59.0466	-60.8754
Pose65	-17.3215	-1.07555	-7.24608	-10.8	-59.658	-63.0426
Pose67	-16.7847	-0.4099	-5.983	-11.4	-61.6342	-60.7989

In our case no bumps were found between receptor and ligand. The detailed lists of the residues involved in hydrogen bonding are shown in Table 3 along with bond distance in angstrom; atoms involved in bonding, DHA angle and HAY angle for all intermolecular H-bonds.

Table 3: Detail of intermolecular H-bond between S100B with Melittin (Pose – 30)

Amino acid residues involved in H-bond formation	Distance	Atom 1	Atom 2	Angle DHA	Angle HAY
Lig:LYS7:HZ2 - Rec:SER41:O	2.03619	HZ2	O	123.802	129.755
Lig:ARG22:HH11- Rec:GLU89:OE2	2.31233	HH11	OE2	117.182	104.193
Lig:ARG22:HH21- Rec:GLU91:OE2	2.12101	HH21	OE2	133.286	114.172
Lig:LYS23:HZ2 - Rec:HIS90:O	2.35982	HZ2	O	111.389	132.055
Lig:LYS23:HZ3- Rec:GLU91:OE1	1.94974	HZ3	OE1	145.459	89.5558
Lig:LYS23:HZ3- Rec:GLU91:OE2	2.15702	HZ3	OE2	143.681	80.576

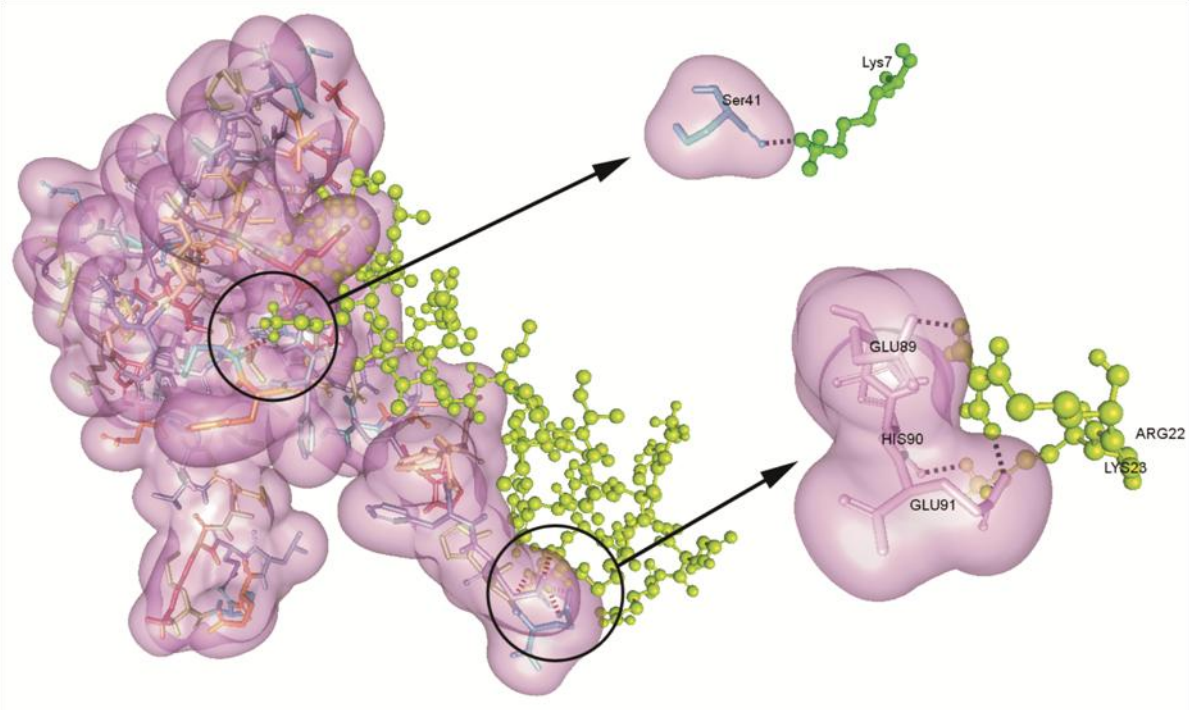

Figure 1 Molecular interactions of S100B and Melittin proteins. Intermolecular hydrogen bonds between S100B and melittin are shown by black color, and the interacting residues in both the proteins are labeled.

3.3 Molecular Dynamics Simulation

In order to evaluate the relative stability of first and the last pose among top 20 poses chosen on the basis of E_RDock score, we performed molecular dynamics simulation studies. Implicit solvent model conditions were created for studying protein peptide simulations. The constant temperature dynamics using Berendsen weak coupling method was applied to examine the potential and total energy differences between the two poses (Figure 2). We observed that the complex in pose 1 was more stable than pose 20. All the persisting hydrogen bonds in two MD simulated complexes (pose 1 and pose 20) were examined from the average structure calculated from 5 ns time scale. We noticed that hydrogen bond formed between S100B:Glu91 and melittin: Lys23 don't remain stable and leaves its contact during simulation.

4. DISCUSSION

Previous studies suggest the over expression of S100B protein associated with many neurodegenerative diseases [25, 26, 27, 28]. Winocur and co-workers observed the hyperactivity and impaired hippocampal functioning in transgenic mice due to S100B over expression [29]. S100B protein has two Ca^{2+} - binding domains in each of its monomer units and upon binding with Ca^{2+} conformational changes has been observed in the S100B leading to the exposure of hydrophobic groups that are necessary for S100B to interact with other proteins in the pathway. The detailed structural and functional insights of Ca^{2+} interaction with S100B calcium binding domain has been previously studied [30]. It was observed that Ca^{2+} ion interaction is coordinated by Ser41 and Leu44 from one subunit and Asp12 of another subunit of S100B. Over expression of S100B resulted in the Ca^{2+} ion imbalance that leads to the disease state.

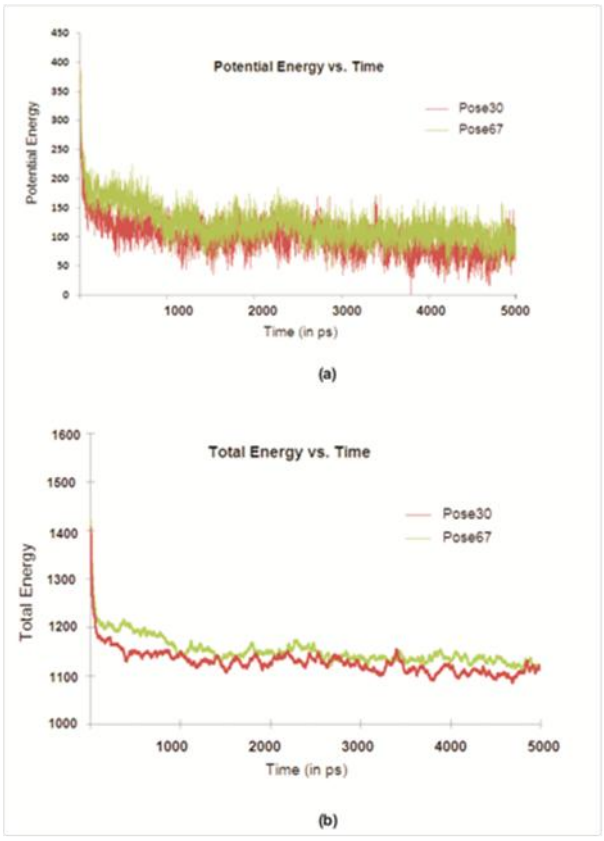

Figure 2 Energy vs. time simulation graphs. (a) Potential and (b) Total energy simulation graph between pose30 and 67 for a total 5ns run.

Our results with melittin and S100B interaction shows that persistent strong hydrogen bonds are formed between 1)

S100B:Glu89 and melittin:Arg22; 2) S100B:Glu91 and melittin:Arg22; 3) S100B:His90 and melittin:Lys23, 4) S100B:Glu91 and melittin:Lys23; and 5) S100B:Ser41 and melittin:Lys7. The simulation studies also revealed the effect of conformational changes of tyrosine residue of melittin which moves to a less polar environment (Figure 3) upon complex formation with S100B as was earlier examined by Baudier and co-workers [18].

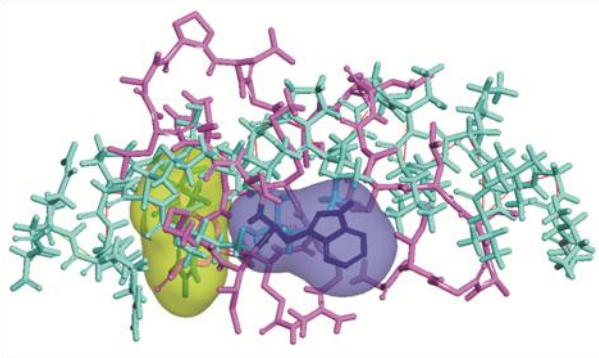

Figure 3 Superposition of melittin before (Cyan) and after (Pink) complex formation with S100B. Also, the significant structural deviation in TRP19 of melittin before (green surface) and after (blue surface) interaction with S100B protein are highlighted.

Structural superposition of melittin before and after complex formation showed very high (8.531 Å) structural deviation (Figure 3), leading to changes in the environment of certain residues including TRP19 of melittin (Figure 4).

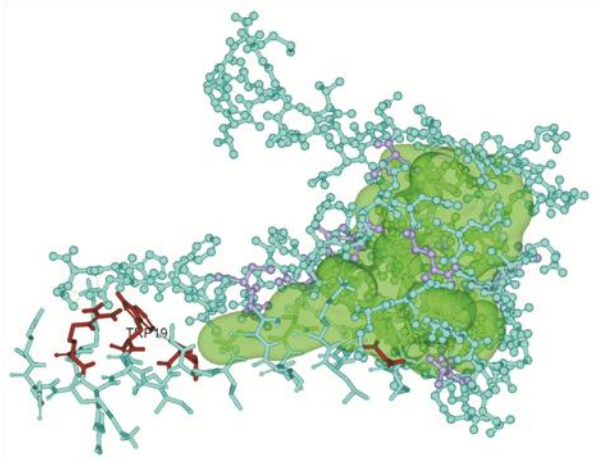

Figure 4 Interaction between S100B and melittin showing exposed (cyan), buried (green) and partial exposed residues including TRP19 of melittin (red).

The interaction of melittin with S100B also interfere and blocks the Ca^{2+} ion binding domain of S100B as amino acid residue Ser41 which coordinate the Ca^{2+} ion binding directly interact with melittin. The interaction of Ser41 from the Ca^{2+} binding domain of S100B with Lys7 of melittin was also stable as we observed throughout the MD simulation run. Our results clearly indicate that melittin from bee venom helps in maintaining the ionic balance which disrupt due to the over expressing of S100B in disease conditions. S100B has been shown not only a prognostic marker, but also to contribute to cancer progression in malignant melanoma by interacting with p53 and inhibiting its function as a tumor suppressor [31, 32, 33]. Therefore, our study also support the hypothesis that melittin has potential to disrupt the normal functioning of S100B hence may be a promising future therapeutics for epilepsy. Few studies also highlight the contribution of S100B in the depletion of wild-type p53 protein in malignant melanoma. The S100B protein levels have been also observed to be elevated in various types of cancers [34]. Thus melittin may also be explored as potential cancer therapeutics.

5. CONCLUSION

S100B over expression has been proposed to play an important in epileptic therapy by increasing calcium concentration and turn on the active phospholipase C and IP3 through activation of various central nervous system neurons. We predict the interaction ability of melittin with S100B using various computational approaches. It was noticed that melittin forms a high-affinity complex with S100B. The conformational changes in the S100B-melittin complex were observed by molecular dynamics simulations. The study revealed that besides the van der Walls interactions, there are some persistent hydrogen bonds that maintain the stability of the complex. Some of the amino acid residues involved in the coordination of Ca^{2+} ion binding in S100B directly interact with melittin. Therefore, melittin has the ability to interfere with S100B protein functionality responsible for epileptogenesis and also tumorigenesis. As the bee venom therapy is in use against epilepsy in some part of the world, these computational studies provide the molecular insights of such traditional therapies that are important to identify the potential drug molecules.

6. ACKNOWLEDGEMENTS

Funding: NV and SS was financially supported by Society for Biological Research & Rural Development. KPS and MK was supported by ENVIS project at CSIR-Indian Institute of Toxicology Research, Lucknow India funded by MoEF, Govt. of India (SSP-0016).

7. REFERENCES

[1] Blume, WT., Lüders, HO., Mizrahi, E., Tassinari, C., van Emde Boas, W., Engel J, Jr., 2001. Glossary of descriptive terminology for ictal semiology: report of the ILAE task force on classification and terminology. Epilepsia. 42, 1212–1218.

[2] Carpio, A., and Hauser, WA., 2009. Epilepsy in the developing world. Curr. Neurol. Neurosci. Rep. 9, 319-326.

[3] Spinella, M. 2001. Herbal Medicines and Epilepsy: The Potential for Benefit and Adverse Effects. Epilepsy Behav. 2, 524-532.

[4] Perucca, E. 2009. What is the promise of new antiepileptic drugs in status epilepticus? Focus on brivaracetam, carisbamate, lacosa-mide, NS-1209, and topiramate. Epilepsia. 50, 49-50.

[5] McCabe, PH. 2000. New anti-epileptic drugs for the 21st century. Expert. Opin. Pharmacother. 1, 633-674.

[6] Johannessen Landmark, C., and Patsalos, PN., 2010. Drug interactions in-volving the new second- and third-generation antiepileptic drugs. Expert. Rev. Neurother. 10, 119-140.

[7] Temkin, NR. 2001. Antiepileptogenesis and seizure prevention trials with antiepileptic drugs: meta-analysis of controlled trials. Epilepsia.42, 515-524.

[8] Schachter, SC. 2002. Current evidence indicates that antiepileptic drugs are anti-ictal, not antiepileptic. Epilepsy Res. 50, 67-70.

[9] Macleod, S., and Appleton, RE., 2007. The new antiepileptic drugs. Arch. Dis. Child Educ. Pract. Ed.92, 182-188.

[10] Mirshafiey. 2007. A Venom therapy in multiple sclerosis. Neuro-pharmacology. 53, 353-361.

[11] Maulet, Y., Mathey-Prevot, B., Kaiser, G., Rüegg, UT., Fulpius, BW., 1980. Purification and Chemical Characterization of Melittin and Acetylated Derivatives. Biochim. Biophys. Acta. 625, 274-80.

[12] Habermann, E., 1972. Bee and Wasp Venom. Science, 177, 314-322.

[13] Miller, RJ., 2001. Rocking and rolling with Ca2+ channels. Trends Neurosci. 24, 445-449.

[14] Van Eldik, LJ., Griffin, WS., 1994. S100 beta expression in Alzheimer's disease: relati on to neuropathology in brain regions. Biochim Biophys Acta. 29, 3398-3403.

[15] Donato, R., 2001. S100: a multigenic family of calcium-modulated proteins of the EF-hand type with intracellular and extracellular functional roles. Int J Biochem Cell Biol. 33, 637-668.

[16] Liu, CH., Lin, YW., Tang, NY., Liu, HJ., Hsieh, CL., 2012. Neuroprotective Effect of Uncaria rhyncho-phylla in Kainic Acid-Induced Epileptic Seizures by Modulating Hippocampal Mossy Fiber Sprouting, Neuron Survival, Astrocyte Proliferation, and S100B Expression. Evid. Based. Complement. Alternat. Med. 2012, 194790.

[17] Gauldie, J., Hanson, JM., Rumjanek, FD., Shipolini, RA., Vernon, CA.1976. The peptide components of bee venom. Eur. J. Biochem. 61, 369-376.

[18] Baudier, J., Mochly-Rosen, D., Newton, A., Lee, SH., Koshland, DE Jr., Cole, RD., 1987. Comparison of S100b protein with calmodulin: interactions with melittin and microtubule-associated tau proteins and inhibition of phosphorylation of tau proteins by protein kinase C. Biochemistry. 26, 2886-2893.

[19] Billeter, SR., Alexander, J., Turner., Walterm, Thiel., 2000. Linear scaling geometry optimization and transition state search in hybrid delocalized internal coordinates. Phys. Chem. 2, 2177-2186.

[20] Chen, R., Weng, ZP., 2002. Docking unbound proteins using shape complementarity, desolvation, and electrostatics. Proteins. 47, 281-294.

[21] Chen, R., Li, L., Weng, Z., 2003. ZDOCK: An Initial-Stage Protein-Docking Algorithm. Proteins. 52, 80–87

[22] Li, L., Chen, R., Weng, Z., 2003. RDOCK: Refinement of rigid-body protein docking predictions. Proteins. 53, 693-707.

[23] Brooks, BR., Bruccoleri, RE., Olafson, BD., States, DJ., Swaminathan, S., Karplus, M., 1983. CHARMm: A program for macromolecular energy, minimization and dynamics calculations. J. Comput. Chem. 4, 187-217.

[24] Momany, FA., and Rone, R.,1992. Validation of the general purpose QUANTA ®3.2/ CHARMm® force field. J comp chem. 13, 888-900.

[25] Heizmann, CW., Günter, Fritz., Beat, W., Schäfer., 2002. S100 Proteins: Structure, Functions and Pathology Frontiers in Bioscience. 7, 1356-1368.

[26] Baudier, J., Cole, RD., 1988. Interactions between the microtubule-associated tau proteins and S100b regulate tau phosphorylation by the Ca2+/calmodulin-dependent protein kinase II. J Biol Chem. 263, 5876-5883.

[27] Sheng, JG., Mrak, RE., Bales, KR., Cordell, B., Paul, SM., Jones, RA., Woodward, S., Zhou, XQ., McGinness, JM., Griffin, WS., 2000. Overexpression of the neuritotrophic cytokine S100beta precedes the appearance of neuritic beta-amyloid plaques in APPV717F mice. J. Neurochem. 74, 295-301.

[28] Sorci, G., Agneletti, AL., Donato, R., 2000. Effects of S100A1 and S100B on microtubule stability. An in vitro study using triton-cytoskeletons from astrocyte and myoblast cell lines. Neuroscience. 99, 773-83.

[29] Winocur, G., Roder, J., Lobaugh, N., 2001. Learning and memory in S100-beta transgenic mice: an analysis of impaired and preserved function. Neurobiol. Learn. Mem. 75, 230-243.

[30] Ostendorp, T., Leclerc, E., Galichet, A., Koch, M., Demling, N., Weigle, B., Heizmann, CW., Kroneck, PM., Fritz, G., 2007. Structural and functional insights into RAGE activation by multimeric S100B. EMBO J. 26, 3868-3878.

[31] Grigorian, M., Andresen, S., Tulchinsky, E., Kriajevska, M., Carlberg, C., Kruse, C., Cohn, M., Ambartsumian, N., Christensen, A., Selivanova, G., Lukanidin, E., 2001. Tumor suppressor p53 protein is a new target for the metastasis-associated Mts1/S100A4 protein: functional consequences of their interaction. J. Biol. Chem. 276, 22699-22708.

[32] Lin, J., Blake, M., Tang, C., Zimmer, D., Rustandi, RR., Weber, DJ., Carrier, F., 2001. Inhibition of p53 transcriptional activity by the S100B calcium-binding protein. J. Biol. Chem. 14, 35037-35041.

[33] Carrier, F., M, Blake., D, Zimmer., Rustandi, RR., Weber, DJ., 1999. Abrogation of p53 transcriptional activity by the S100 calcium binding proteins: Possible implication in angiogenesis. Proc. AACR. 40, 102.

[34] Wilder, PT., Lin, J., Bair, CL., Charpentier, TH., Yang, D., Liriano, M., Varney, KM., Lee, A., Oppenheim, AB., Adhya, S., Carrier, F., Weber, DJ., 2006. Recognition of the tumor suppressor pro-tein p53 and other protein targets by the calcium-binding protein S100B. Biochim. Biophys. Acta. 1763, 1284-1297.